

**HORSESHOE CHAOS IN A PERIODICALLY
PERTURBED POLARIZED OPTICAL BEAM**

By

D. DAVID

D. D. Holm

and

M.V. Tratnik

IMA Preprint Series # 488

February 1989

Horseshoe Chaos in a Periodically Perturbed Polarized Optical Beam

D. David, D. D. Holm, and M. V. Tratnik[†]
Institute for Mathematics and its Applications,
University of Minnesota, Minneapolis, MN 55455.

Abstract

The problem of a single, polarized, laser pulse propagating as a travelling wave in an anisotropic cubically nonlinear, lossless medium is investigated as a Hamiltonian system. This Hamiltonian system describes the travelling-wave dynamics of two nonlinearly coupled complex laser modes. Invariance of the Hamiltonian function under changes of phase of the complex two-component electric field amplitude reduces the phase space to the two-sphere, S^2 , on which the problem is completely integrable. The fixed points and bifurcations of the phase portrait on S^2 are studied as the beam intensity and medium parameters are varied, and homoclinic and heteroclinic connections are identified in each parameter domain. Horseshoe chaos is analytically shown to arise when the optical parameters of the medium are perturbed due to spatially periodic inhomogeneities, by using the Melnikov method. The resulting sensitive dependence on initial conditions has implications for the control and predictability of nonlinear optical polarization switching in birefringent media.

1. Introduction.

This paper treats optical polarization dynamics, using the Stokes description ^[1] for a single laser pulse propagating as a travelling wave in an anisotropic cubically nonlinear lossless medium. Hamiltonian methods are used to reduce the phase space C^2 (the two-component, complex-vector electric field amplitude) for the travelling-wave dynamics to the spherical surface S^2 (the Poincaré sphere). Bifurcations of the phase portrait on S^2 are determined, and homoclinic and heteroclinic orbits connecting hyperbolic fixed points are identified. These homoclinic and heteroclinic orbits are separatrices, i.e., stable and unstable manifolds of hyperbolic fixed points, which separate regions on S^2 having different types of (periodic) behavior. Under spatially periodic perturbations of the medium parameters, the stable and unstable manifolds are shown to tangle and produce a Smale horseshoe in the Poincaré map induced from the periodic perturbation. The presence of this tangle is diagnosed via the Melnikov method, which identifies intersections of these stable and unstable manifolds and estimates the width of the tangled region on S^2 . The analysis presented here characterizes the location of the chaotic set, or stochastic layer, on the Poincaré sphere and the dependence of its width on the material parameters, spatial modulation amplitude and wavelength, and the optical beam intensity.

[†]: Permanent address: Center for Nonlinear Studies & Theoretical Division, MS B258,
Los Alamos National Laboratory, Los Alamos, NM 87545.

1. Problem formulation.

Propagation of an optical travelling wave pulse in a cubically nonlinear medium is described by the following system of equations [2, 3],

$$i \frac{d}{d\tau} e_j = \chi_{jk}^{(1)} e_k + 3\chi_{jklm}^{(3)} e_k e_l e_m^* \quad (2.1)$$

where τ is the independent variable for travelling waves, $j, k, l, m = 1, 2$, and the complex two-vector $e = (e_1, e_2)^T \in \mathbb{C}^2$ represents the electric field amplitude. The complex susceptibility tensors $\chi_{jk}^{(1)}$ and $\chi_{jklm}^{(3)}$ parametrize the linear and nonlinear polarizability, respectively. Far from resonance and in a lossless medium, the susceptibility tensors are constant and Hermitian in each e - e^* pair and $\chi^{(3)}$ possesses a permutation symmetry:

$$\chi_{jk}^{(1)} = \chi_{kj}^{(1)*}, \quad \chi_{jklm}^{(3)} = \chi_{kjml}^{(3)*}, \quad \chi_{jklm}^{(3)} = \chi_{mklj}^{(3)} = \chi_{jlk m}^{(3)}. \quad (2.2)$$

Hence, we may write the system (2.1) in Hamiltonian form as

$$\begin{aligned} \partial e_j / \partial \tau &= \{e_j, H\}_{\mathbf{c}^2} = -i \partial H / \partial e_j^*, \\ H &\equiv e_j^* \chi_{jk}^{(1)} e_k + \frac{3}{2} e_j^* e_k \chi_{jklm}^{(3)} e_l e_m^*. \end{aligned} \quad (2.3)$$

In addition, the intensity, $r = |e|^2 = |e_1|^2 + |e_2|^2$. We introduce the three-component Stokes vector, \mathbf{u} , given by (see ref. [4]) $\mathbf{u} = e_j^* (\sigma)_{jk} e_k$, with $\sigma = (\sigma_1, \sigma_2, \sigma_3)$, the standard Pauli matrices. The travelling wave equation (2.1) then becomes

$$\frac{d\mathbf{u}}{d\tau} = (\mathbf{b} + \mathbf{W} \cdot \mathbf{u}) \times \mathbf{u}, \quad \mathbf{b} = \mathbf{a} + |\mathbf{u}| \mathbf{c} = \mathbf{a} + r \mathbf{c}, \quad (2.4)$$

where the constant vectors \mathbf{a} and \mathbf{c} , and the constant symmetric tensor \mathbf{W} , are given by

$$\mathbf{a} = (\sigma)_{kj} \chi_{jk}^{(1)}, \quad \mathbf{c} = \frac{3}{2} (\sigma)_{kj} \chi_{jklm}^{(3)}, \quad \mathbf{W} = \frac{3}{2} (\sigma)_{kj} \chi_{jklm}^{(3)} (\sigma)_{lm} = \text{diag}(\lambda_1, \lambda_2, \lambda_3). \quad (2.5)$$

The material parameters \mathbf{a} , \mathbf{c} , and \mathbf{W} are all real. According to equation (2.5), the parameters \mathbf{a} and \mathbf{c} represent the effects of linear and nonlinear anisotropy, respectively. They lead to precession of the Stokes vector \mathbf{u} with (vector) frequency \mathbf{b} . The tensor \mathbf{W} is symmetric, so a polarization basis may always be assumed in which \mathbf{W} is diagonal, $\mathbf{W} = (\lambda_1, \lambda_2, \lambda_3)$, in analogy to the principal moments of inertia of a rigid body.

In terms of the Stokes parameters, \mathbf{u} , the Hamiltonian function H in equation (2.5) may be rewritten as

$$\mathbf{H} = \mathbf{b} \cdot \mathbf{u} + \frac{1}{2} \mathbf{u} \cdot \mathbf{W} \cdot \mathbf{u} \quad (2.6)$$

and the equations of motion (2.9) may be expressed in Hamiltonian form as $d\mathbf{u}/d\tau = \{\mathbf{u}, H\}$, by using the Lie-Poisson bracket $\{F, G\} := \mathbf{u} \cdot \nabla F(\mathbf{u}) \times \nabla G(\mathbf{u})$ written in triple scalar product form, just as in the case of the rigid body. The intensity $r = |\mathbf{u}|$ is the Casimir function for this Lie-Poisson bracket. That is, r Poisson-commutes with all functions of \mathbf{u} when the above Lie-Poisson bracket is used; so the intensity r in the Stokes description of lossless polarized optical beam dynamics may be regarded simply as a constant parameter. (See ref. [5] for discussions and references concerning Lie-Poisson brackets and their usage, for example, in the study of Lyapunov stability of equilibrium solutions of dynamical systems.)

Solving the system (2.4) when two eigenvalues of W coincide, and one or more of the components of b vanish, can be done easily for two cases which are inequivalent under cyclic permutations of indices of u . In the first case, we set $W = \omega \text{diag}(1, 1, 2)$ and $b = (b_1, b_2, 0)$; equations (2.4) then read

$$du_1/d\tau = (b_2 - \omega u_2)u_3, \quad du_2/d\tau = (\omega u_1 - b_1)u_3, \quad du_3/d\tau = b_1 u_2 - b_2 u_1. \quad (2.7)$$

Hence, a Duffing equation emerges for u_3 ,

$$d^2 u_3 / d\tau^2 = A u_3 (B - u_3^2), \quad (2.8)$$

$$A = \frac{1}{2} \omega^2, \quad B = \frac{2H}{\omega} - r^2 - \frac{2(b_1^2 + b_2^2)}{\omega^2}.$$

The other two components of u may be determined algebraically from the two constants of motion r and H . When B increases through zero, the Duffing equation (2.8) develops a pair of orbits, homoclinic to the fixed point u_3 (see, e.g., refs. [6] and [7]). Likewise, in the second case, we set $W = \omega \text{diag}(1, 1, 2)$ and $b = (b_1, 0, b_3)$; equations (2.4) then become

$$du_1/d\tau = -b_3 u_2 - \omega u_2 u_3, \quad du_2/d\tau = \omega u_1 u_3 + b_3 u_1 - b_1 u_3, \quad du_3/d\tau = b_1 u_2. \quad (2.9)$$

Hence, provided $b_1 \neq 0$, we find

$$d^2 u_3 / d\tau^2 = A' + B' u_3 + C' u_3^2 + D' u_3^3, \quad (2.10)$$

$$A' = b_3 (H - \frac{1}{2} \omega r^2), \quad B' = \omega H - \frac{1}{2} \omega^2 r^2 - b_1^2 - b_3^2, \quad C' = -\frac{3}{2} \omega b_3, \quad D' = -\frac{1}{2} \omega^2.$$

Thus, the polarization dynamics for this case reduces to the motion of a particle in a quartic potential, whose solution is expressible in terms of elliptic integrals. Again, the components u_1 and u_2 may be determined algebraically from the two constants of motion, r and H . We shall return to these two cases later, when we discuss the effects of perturbations. For now, these cases suffice to demonstrate that the system (2.4) possesses bifurcations in which homoclinic orbits are created.

The system of equations (2.9) further reduces the Poincaré sphere Σ_r of radius r upon transforming to spherical coordinates $(u_1, u_2, u_3) = (r \sin \theta \sin \varphi, r \cos \theta, r \sin \theta \cos \varphi)$. In these coordinates, the reduced Hamiltonian function (2.6) and the symplectic Poisson bracket on Σ_r are expressible as

$$H = \frac{1}{2} r^2 (\lambda_1 \sin^2 \theta \sin^2 \varphi + \lambda_2 \cos^2 \theta + \lambda_3 \sin^2 \theta \cos^2 \varphi) + r \sin \theta (b_1 \sin \varphi + b_3 \cos \varphi) + b_2 r \cos \theta, \quad (2.11)$$

$$(F, G) := \frac{1}{r} \frac{\partial F}{\partial \varphi} \frac{\partial G}{\partial \cos \theta} - \frac{1}{r} \frac{\partial F}{\partial \cos \theta} \frac{\partial G}{\partial \varphi}.$$

and the equations of motion are

$$d\theta/d\tau = b_1 \cos \varphi - b_3 \sin \varphi + (\lambda_1 - \lambda_3) r \sin \theta \cos \varphi \sin \varphi, \quad (2.12)$$

$$d\varphi/d\tau = b_2 - (b_1 \sin \varphi + b_3 \cos \varphi) \cot \theta - r (\lambda_1 \sin^2 \varphi + \lambda_3 \cos^2 \varphi - \lambda_2) \cos \theta.$$

The system (2.9) is completely integrable, since it is a one-degree-of-freedom Hamiltonian system. Its solutions in general are expressible in terms of elliptic integrals.

3. Bifurcation analysis.

We now specialize to the case of a non-parity invariant material with C_4 rotation symmetry about the axis of propagation (the z-axis), for which material constants take the form $W = (\lambda_1, \lambda_2, \lambda_3)$ and $b = (0, b_2, 0)$. (see ref. [8] for details of what follows.) We also introduce the following parameters

$$\mu = \lambda_3 - \lambda_1, \quad \lambda = (\lambda_2 - \lambda_1)/(\lambda_3 - \lambda_1), \quad \beta = b_2/[r(\lambda_3 - \lambda_1)]. \quad (3.1)$$

In this case, the Hamiltonian in (2.11) and the equations of motion become

$$H = \frac{1}{2}\mu[(r^2 - u^2)\cos^2\varphi + \lambda u^2 + 2\beta ru] + \frac{1}{2}\lambda_1 r^2, \quad (3.2a)$$

$$du/d\tau = \mu(r^2 - u^2)\cos\varphi\sin\varphi, \quad (3.2b)$$

$$d\varphi/d\tau = \mu[\beta r - (\cos^2\varphi - \lambda)u], \quad (3.2c)$$

where $u = r\cos\theta$. We construct the phase portrait of the system and explain how this portrait changes as the parameters in the equations vary. The fixed points of (3.2b,c) are easily located and classified, using standard techniques. We list them in the following table, for $\mu \neq 0$.

Fixed Point	Coordinates	Constraint	Saddle	Center
F	$\varphi = 0 \quad \cos\theta = \beta/(1 - \lambda)$	$\beta^2 < (1 - \lambda)^2$	$\lambda > 1$	$\lambda < 1$
B	$\varphi = \pi \quad \cos\theta = \beta/(1 - \lambda)$			
L	$\varphi = \pi/2 \quad \cos\theta = \beta/\lambda$	$\beta^2 < \lambda^2$	$\lambda < 0$	$\lambda > 0$
R	$\varphi = -\pi/2 \quad \cos\theta = \beta/\lambda$			
N	$\cos^2\varphi = \lambda + \beta \quad \theta = 0$	—	$\beta \in (-\lambda, 1 - \lambda)$	$\beta \notin (-\lambda, 1 - \lambda)$
S	$\cos^2\varphi = \lambda - \beta \quad \theta = \pi$	—	$\beta \in (\lambda - 1, \lambda)$	$\beta \notin (\lambda - 1, \lambda)$

Table. The fixed points of system (3.2) and their types.

The special case where $\mu = 0$, i.e., $\lambda_3 = \lambda_1$, requires a separate analysis. In that case, the right-hand side of (1.4a) vanishes identically so that the set of fixed points of the system is the circle $\cos\theta = b_2/r(\lambda_2 - \lambda_1) = \beta/\lambda$. The phase portrait depends on two essential parameters, λ and β , or equivalently, $\lambda_2 - \lambda_1$ and b_2/r . Bifurcations of the phase portrait occur when the inequality constraints in the third column of the above table become equalities; hence we observe that the pairs of fixed points (F, B) and (L, R) appear or vanish as the lines $\beta = \pm(1$

$-\lambda$) and $\beta = \pm\lambda$ are crossed in the (λ, β) parameter plane (see Figure 1):

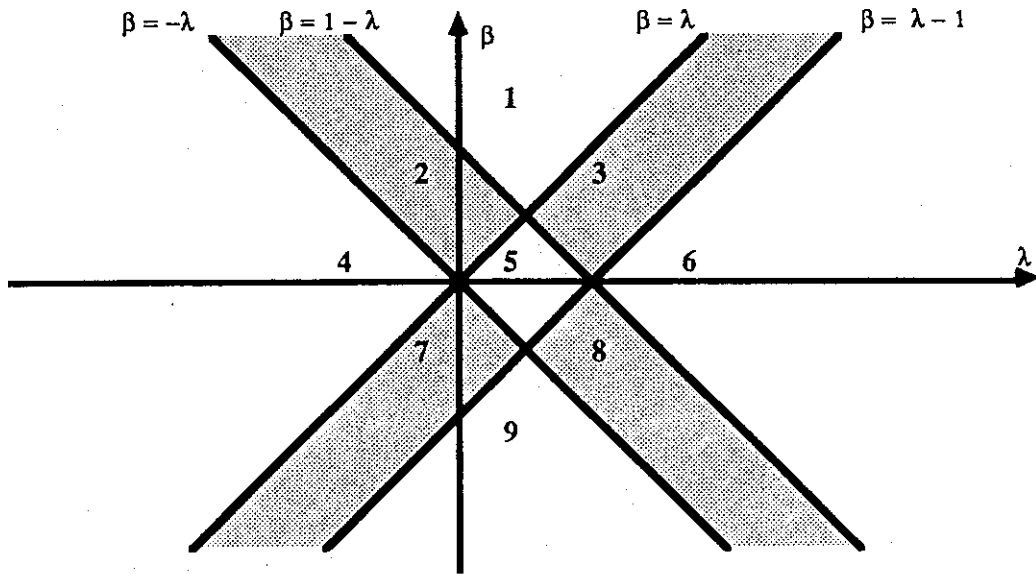


Figure 1. The parameter plane and its bifurcation lines.

The (λ, β) parameter plane is partitioned into nine distinct regions separated by four critical lines that intersect in pairs at four points. Typical phase portraits corresponding to each of these regions are shown in Figure 2. Note that the phase portraits of the unperturbed system (3.2b,c) are invariant under the following discrete transformations:

$$\begin{array}{ll} \varphi \rightarrow \varphi \pm \pi; & \varphi \rightarrow \varphi \pm \pi, \theta \rightarrow \pi - \theta, \beta \rightarrow -\beta; \\ \varphi \rightarrow \varphi \pm \pi/2, \lambda \rightarrow 1 - \lambda, \beta \rightarrow -\beta; & \varphi \rightarrow \varphi \pm \pi/2, \lambda \rightarrow 1 - \lambda, \theta \rightarrow \pi - \theta. \end{array}$$

Thus, as far as the configurations of critical orbits on the phase sphere are concerned, it will be sufficient to consider the quarter plane given by $\lambda < 1/2$ and $\beta > 0$, i.e., to restrict attention to regions 1, 2, 4, and 5. Although no bifurcations occur when the λ -axis ($\beta = 0$ in the parameter plane) is crossed (except for $\lambda = 0$, and $\lambda = 1$, the set of fixed points does not change), this line is nevertheless special. Indeed, in the interval $\lambda \in (0, 1)$, i.e. within region R5, both poles are hyperbolic, each one of them being attached to a pair of homoclinic loops. When β vanishes, these homoclinic loops merge together so as to form four heteroclinic lines (and thus four heteroclinic 2-cycles) connecting the north and south poles together. On the λ -axis the polarization dynamics reduces to that of the rigid body. In that case, the phase portrait consists of the poles N and S, and the four other points are located on the equator of S^2 (this configuration of fixed points distributed on the equator is obtained only on this line). Two of these, (N, S) or (F, B) or (R, L), are unstable while the other four are stable; which pair is unstable is decided by the value of $\lambda = (\lambda_2 - \lambda_1)/(\lambda_3 - \lambda_1)$. The pair (F, B) is hyperbolic when $\lambda < 0$, (N, S) are hyperbolic when $0 < \lambda < 1$, and (R, L) are hyperbolic whenever $\lambda > 1$; in each of these cases, the unstable direction is specified by the λ_i which is neither the smallest or the greatest among the three.

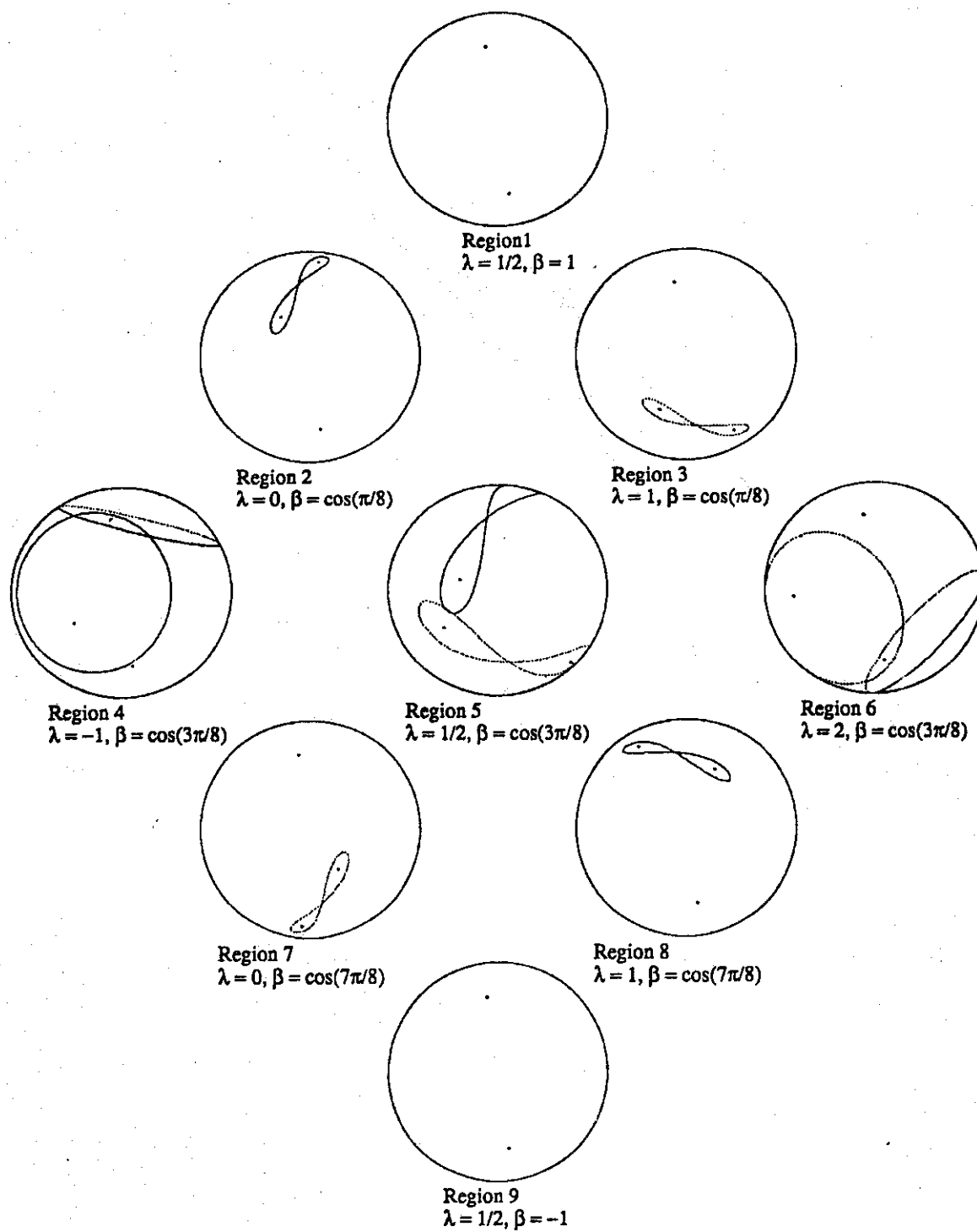


Figure 2. Phase portraits of system (3.2)

Bifurcations taking place as the beam intensity is varied are those occurring along a vertical line in the parameter plane; we present a list of the seven possible sequences (see ref. [8] for an exhaustive list of the bifurcations that may take place in the phase plane when travelling along these lines):

$S_1:$	$\lambda < 0$	$R1 \leftrightarrow R2 \leftrightarrow R4 \leftrightarrow R7 \leftrightarrow R9$
$S_2:$	$\lambda = 0$	$R1 \leftrightarrow R2 \leftrightarrow R7 \leftrightarrow R9$
$S_3:$	$0 < \lambda < 1/2$	$R1 \leftrightarrow R2 \leftrightarrow R5 \leftrightarrow R7 \leftrightarrow R9$
$S_4:$	$\lambda = 1/2$	$R1 \leftrightarrow R5 \leftrightarrow R9$
$S_5:$	$1/2 < \lambda < 1$	$R1 \leftrightarrow R3 \leftrightarrow R5 \leftrightarrow R8 \leftrightarrow R9$
$S_6:$	$\lambda = 1$	$R1 \leftrightarrow R3 \leftrightarrow R8 \leftrightarrow R9$
$S_7:$	$\lambda > 1$	$R1 \leftrightarrow R3 \leftrightarrow R6 \leftrightarrow R8 \leftrightarrow R9$

4. Homoclinic chaos.

In this section, we consider spatially periodic modulations of either the circular-circular polarization self-interaction coefficient λ_2 in W or the optical activity b_2 . In each case, when the unperturbed medium satisfies the additional condition $\lambda_2 = \lambda_3$, the Melnikov technique [6,7,9] leads to an analytically manageable integral for the Melnikov function, which is shown to have simple zeros. In this way, horseshoe chaos is predicted for this case in the dynamics of the single Stokes pulse. We also discuss the physical implications for measuring this horseshoe chaos in an experimental situation.

We concentrate on the north pole $u_2 = 1$, $\varphi = \varphi_0$, with $\cos^2 \varphi_0 = \lambda + \beta$, and evaluate the conserved Hamiltonian at this point to find a relation between u and φ on the homoclinic orbit,

$$u_2 = -r - 2b_2/\mu(\cos^2 \varphi - \lambda), \quad (4.1)$$

which, when substituted into the equation of motion for φ , gives

$$d\varphi/d\tau = \mu r [\cos^2 \varphi - \cos^2 \varphi_0]. \quad (4.2)$$

Upon integrating (4.2) we obtain (with $\tau = z + vt$, the travelling-wave variable)

$$\tan \varphi = \tan \varphi_0 / \tanh(\zeta \tau), \quad \zeta = \frac{1}{2} \mu r \sin(2\varphi_0). \quad (4.3)$$

Substituting this formula into (4.1) gives an analytical expression for u on the homoclinic orbit:

$$u_2 = -r - \frac{2b_2[1 - \cos^2 \varphi_0 \operatorname{sech}^2(\zeta \tau)]}{\mu \{ \cos^2 \varphi_0 \tanh^2(\zeta \tau) - \lambda [1 - \cos^2 \varphi_0 \operatorname{sech}^2(\zeta \tau)] \}}. \quad (4.4)$$

We consider a periodic perturbation of the eigenvalue λ_2 and the optical activity b_2 , that is,

$$\lambda_2' = \lambda_2 + \varepsilon_1 \cos(vz), \quad b_2' = b_2 + \varepsilon_2 \cos(vz), \quad (4.5)$$

where $\varepsilon_{1,2} \ll 1$ and v is the modulation frequency. Then from (2.6) the perturbation Hamiltonian is

$$H^1 = \frac{1}{2} u_2 (\varepsilon_1 u_2 + 2\varepsilon_2) \cos(vz). \quad (4.6)$$

and we easily calculate the Poisson bracket of this perturbation with the unperturbed Hamiltonian:

$$\{H^0, H^1\} = -\mu \sin\varphi \cos\varphi (r^2 - u_2^2) u_2 \cos(vz), \quad (4.7)$$

which when formally integrated becomes the Melnikov function

$$M(\tau_0) = \mu \int_{\mathbf{R}} \sin\varphi(\tau) \cos\varphi(\tau) (r^2 - u_2^2(\tau)) (\varepsilon_1 u_2 + \varepsilon_2) \cos[v(\tau - \tau_0)] d\tau, \quad (4.8)$$

where $\tau_0 = vt$. In the particular case $\lambda_2 = \lambda_3$, this integrable is manageable and can be found in standard tables. Hence,

$$M(\tau_0) = \frac{2\pi v^2}{b_2^2} \left[r(\varepsilon_1 r + \varepsilon_2) + \frac{2}{3} \varepsilon_1 r^2 \{ \cos^2 \varphi_0 + (v/2b_2)^2 \} \right] \text{csch}[v\pi/\mu r \sin(2\varphi_0)] \sin(v\tau_0), \quad (4.9)$$

which clearly has simple zeros as a function of τ_0 , implying horseshoe chaos (see, e.g., refs. [6] and [7]). When the Melnikov function has simple zeros, the dynamical evolution of a rectangular region near the homoclinic point shows (under iteration of the Poincaré map induced from the periodic perturbation) that the region is folded, stretched, contracted, and eventually mapped back over itself in the shape of a horseshoe. This horseshoe map is the underlying mechanism for chaos. As the horseshoe folds and refolds, the rectangular region of phase points initially lying near the homoclinic point develops a Cantor set structure whose associated Poincaré Map can be shown to contain countably many unstable periodic motions, and uncountably many unstable nonperiodic motions. (See ref. [7] for the methods of proof of these statements and further descriptions of hamoclinic tangles.)

5. Conclusions.

Physically, the horseshoe chaos in the case of a periodically perturbed single Stokes pulse corresponds to intermittent switching from one elliptical polarization state, to another one whose semimajor axis is approximately orthogonal to that of the first state, with a passage close to the unstable circular polarization state during each switch. This intermittency is realized on the Poincaré sphere by an orbit which spends most of its time near the unperturbed *figure eight* shape with a (homoclinic) crossing at the north pole (circular polarization) in Figure 2. Under periodic perturbations of either the *W*-eigenvalues or the optical activity b_2 , this orbit switches deterministically, but with extreme sensitivity to the initial conditions, from one lobe of the figure eight to the other each time it returns to the crossing region near the north pole where the homoclinic tangle is located. Thus, for the one-beam problem we predict intermittent and practically unpredictable switching under spatially periodic perturbations of the material parameters, as the optical polarization state passes through a homoclinic tangle near the circular polarization state.

From considerations of the special case in which the Duffing equation (2.8) appears, one could have expected homoclinic chaos to develop for nonlinear optical polarization dynamics. Indeed, a related special case

is studied numerically by Wabnitz [10]. As opposed to such numerical studies, our analytical treatment explored the bifurcations available to the polarization dynamics under the full range of material parameter variations, demonstrated that the horseshoe construct is the mechanism driving the chaotic behavior, and characterized the location of the chaotic set, or stochastic layer, and the dependence of its width on the material parameters, modulation frequency, and intensity.

In the cases under consideration, this stochastic layer is bounded by KAM (Kolmogorov-Arnold-Moser) curves on the Poincaré sphere, inside of which the travelling-wave dynamics is regular (orbitally) and stable. For a given choice of beam and material parameters, those KAM curves define phase space regions where chaotic behavior (for example, sensitive dependence on initial conditions, or orbital instability) may be found, and complementary regions where chaos is absent and only regular, predictable behavior may be found.

The strong dependence on intensity of the phase-space portraits reported here indicates that control and predictability of optical polarization in nonlinear media may become an important issue for future research. In particular, the sensitive dependence on initial conditions in nonlinear polarization dynamics found here to be induced by spatial inhomogeneities may have implications for the control and predictability of optical polarization switching in birefringent media. For instance, an output-output polarization experiment input conditions lying in the stochastic layer for some set of material and beam parameters will show essentially random output after sufficient propagation length, depending on the size of the material inhomogeneities and the type of (transparent) material used for the experiment. Effects on optical polarization dynamics of dissipation and driving, as well as more general material description are presently investigated and will appear elsewhere.

This paper was written during our stay at the University of Minnesota *Institute for Mathematics and its Applications* during fall, 1988, and we wish to thank the IMA for their invitation and their hospitality. We would also like to thank S. Wiggins, A.V. Mikhailov and Y. Kodama for stimulating scientific discussions of this work during our stay at the IMA. Two of us (D.D. and M.V.T.) acknowledge postdoctoral fellowships from the *National Science and Engineering Research Council* of Canada.

6. References.

- [1] M. Born and E. Wolf [1959], *Principle of Optics*, Pergamon Press, Oxford.
- [2] Y.R. Shen [1984], *The Principles of Nonlinear Optics*, Wiley-Interscience, New York.
- [3] N. Bloembergen [1965], *Nonlinear Optics*, Benjamin, New York.
- [4] D. David, D.D./ Holm, and M.V. Trtnik [1988], Hamiltonian chaos in nonlinear optical polarization dynamics, Preprint LA-UR-88-1889, Los Alamos National Laboratory.
- [5] D.D. Holm, J.E. Marsden, T. Ratiu, and A. Weinstein [1987], Nonlinear stability of fluid and plasma equilibria, *Physics Reports* **123**, 1-116.
- [6] J. Guckenheimer and P. Holmes [1983], *Nonlinear Oscillations, Dynamical Systems, and Bifurcations of*

Vector Fields, Springer-Verlag, New York.

- [7] S. Wiggins [1988], *Global Bifurcations and Chaos - Analytical Methods*, Springer-Verlag, New York.
- [8] D. David [1989], Chaotic dynamics in a polarized optical beam submitted to periodic and dissipative Perturbations, Preprint IMA # 487, University of Minnesota.
- [9] V.K. Melnikov [1963], On the stability of the center for time periodic perturbations, *Trans. Moscow Math. Soc.* **12**, 1-57.
- [10] S. Wabnitz [1987], Spatial chaos in the polarization for a birefringent optical fiber with periodic coupling, *Phys. Rev. Lett.* **58**, 1415-1418. This reference notes that Eq. (2.4) also describes the classical dynamics of a single spin in a modulated magnetic field, and refers to K. Nakamura, Y. Okazaki, and A.R. Bishop, *Phys. Rev. Lett.* **57**, 5 (1986).